Contents

Todo list

I Introduction

In 1894, Albert Michelson remarked that "it seems probable that most of the grand underlying principles have been firmly established"[1] [1, p. 159].

What to put in introduction?

At the end of the 19th and the beginning of the 20th century, cooling technology made great progress. Liquifying gases, were able to reach temperatures as low as 4 K (the boiling point of Helium). Using that, SC was discovered in mercury in 1911 by Heike Onnes [2]. Superconductivity describes the phenomenon of the electrical resistance of a material suddenly dropping to zero below a critical temperature T_C. Discovery of Meissner effect, perfect expulsion of external magnetic fields in 1933 [3]. This started almost half a century of intensive theoretical research, which culminated in John Bardeen, Leon Cooper and J. Robert Schrieffer developing the microscopic theory now know as BCS theory [4]. 1986 and 1987: discovery of superconductivity with very high T_C found in cuprates [5, 6]. Cuprate superconductors are made up of layers of cooper oxide and charge reservoirs in between. The specific charge reservoir layers determine the properties of the SC and varying them lead to a rich zoo of materials with high T_C [7].

Largest commercial application to date is in magnetic resonance imaging, a medical technique using strong magnetic fields and field gradients [8]. Enabled due to the fact, that SCs can carry much stronger currents and thus generate much higher magnetic field strength. Technical applications in research are much wider, ranging from strong superconducting magnets in the LHC [9] and other particle accelerators over detectors of single photons in astrophysics [10] to extremely sensitive measurement devices for magnetic fields [11] and voltages [12] based on the Josesphon effect [13].

Since the first discovery of SC in cuprates, there has been a lot of work to develop superconductors with higher transition temperatures. One interesting development in is in twisted multilayer systems, first realized as twisted bilayer

[1] Variations of this quote have been attributed to Lord Kelvin, although the poetry having it said by someones, whose experiment would eventually lead to the development of special relativitiy is undeniable.

Graphene [14]. In comparison to the complex crystal structure of e.g. the Cuprates, twisted multilayer systems have a very simple structure and can be tuned very easily: the angle of twist between the layers can be easily accessed experimentally. The defining feature of these systems are flat electronic bands due to folding of the Brilluoin zone. Superconductivity in these systems is enhanced due to the fact that in the flat bands, interactions between the electrons are very strongly enhanced. Thus these systems are a very interesting playground to study strongly correlation effects in general and superconductivity in particular.

What I am doing: calculating length scales, why is that important?

II Superconductivity

Superconductivity is an example of an emergent phenomenon: the Schrödinger equation describing all interactions between electrons gives no indication that there exists parameters for which the electrons condense into phase coherent pairs. In this chapter we review theoretical concepts needed for understanding superconductivity and introduce the tools used to study superconductivity in the later chapters. There are many textbooks covering these topics which can be referenced for a more detailed treatment, such as refs. [15–19].

Macroscopially, the superconducting state can be described by a spontaneous breaking of a $U(1)$ phase rotation symmetry that is associated with an order parameter. Theory of spontaneous symmetry breaking and associated phase transitions is Ginzburg-Landau theory discussed in section II.1. Ginzburg-Landau theory introduces two length scales: the coherence length ξ describing

Section II.1 also introduces the theoretical framework based on introducing a finite momentum for the Cooper pairs [20] that will be used in later chapters to calculate these length scales from microscopic theories.

Ginzburg Landau theory is not a macroscopic theory, but it can be connected to microscopic theories: if a theory finds an expression for the order parameter describing the symmetry breakdown, it can be connected to quantities expressed by Ginzburg-Landau theory, such as the superconducting current. One such theory to describe superconductivity from a microscopic perspective is BCS (Bardeen-Cooper-Schrieffer) theory in section II.2.

A method to treat local interactions non-perturbatively is DMFT (Dynamical Mean Field Theory). Section II.3 briefly introduces the Greens function method to treat many-body problems and outlines the DMFT self-consistency cycle.

II.1 Ginzburg-Landau Theory of Superconductivity

This review partially follows the introduction given in refs. [15, 21].

Introduction with more history and what will be tackled in this section

II.1.1 Sponteneous Symmetry Breaking and Order Parameter

Symmetries are a powerful concept in physics. Noethers theorem [22] connects the symmetries of physical theories to associated conservation laws. An interesting facet of symmetries in physical theories is the fact, that a ground state of a system must not necessarily obey the same symmetries of its Hamiltonian, i.e. for a symmetry operation that is described by a unitary operator U, the Hamiltonian commutes with U (which results in expectation values of the Hamiltonian being invariant under the symmetry operation) but the states $|\phi\rangle$ and $U|\phi\rangle$ are different. This phenomenon is called SSB (Sponteneous Symmetry Breaking) and the state $|\phi\rangle$ is said to be symmetry-broken.

One consequence of this fact is that for a given symmetry-broken state $|\phi\rangle$, there exists multiple states that can be reached by repeatedly applying U to $|\phi\rangle$ and all have the same energy. To differentiate the symmetry-broken states an operator can be defined that has all these equivalent states as eigenvectors with different eigenvalues and zero expectation value for symmetric states. This is the microscopic notion of an order parameter.

The original notion of an order parameter was motivated from macroscopic observables that can then be related to the microscopic order parameter operator introduced above. Macroscopically we characterize the symmetry breaking by an order parameter Ψ which generally can be a complex-valued vector that becomes non-zero below the transition temperature T_C

$$|\Psi| = \begin{cases} 0 & T > T_C \\ |\Psi_0| > 0 & T < T_C \end{cases} . \tag{II.1}$$

In the example of a ferromagnet, a finite magnetization of a material is associated with a finite expectation value for the z-component of the spin operator, $m_z = \langle \hat{S}_z \rangle$. The order parameter describes the 'degree of order' [23]. Similarly to a magnetically ordered state, the SC state is characterized by an order parameter. The theory of phase transitions in superconductors was developed by Ginzburg and Landau [24]. Landau theory and conversely Ginzburg-Landau theory is not concerned with the the microscopic properties of the order parameter, but describes the changes in thermodynamic properties of matter with the development of an order parameter.

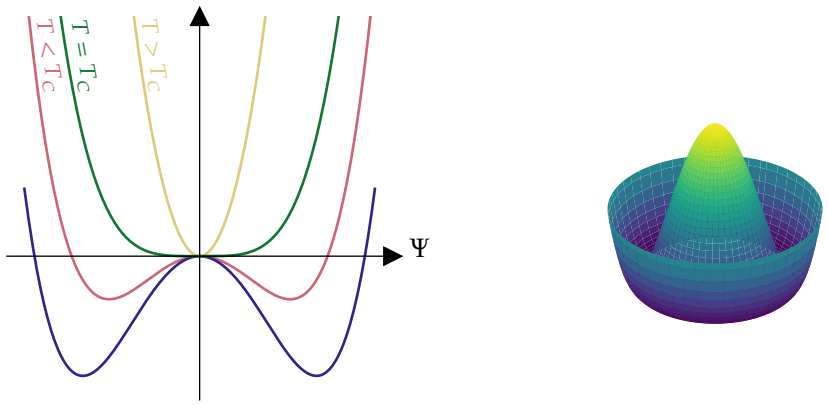

(a) (b)

Figure II.1: *(a) Landau free energy and (b) Mexican hat potential*

II.1.2 Landau and Ginzburg-Landau Theory

The free energy is a thermodynamic quantity:

$$F = E - TS \tag{II.2}$$

with the energy of the system E, temperature T and entropy S. A system in thermodynamic equilibrium has minimal free energy. The fundamental idea underlying Landau theory is to write the free energy $F[\Psi]$ as function of the order parameter Ψ and expand it as a polynomial:

$$F[\Psi] = \frac{r}{2}\Psi^2 + \frac{u}{4}\Psi^4 \,. \tag{II.3}$$

Provided the parameters r and u are greater than 0, there is a minimum of $F[\Psi]$ that lies at $\Psi = 0$. Landau theory assumes that at the phase transition temperature T_C the parameter r changes sign, so it can be written in first order as

$$r = a(T - T_C) \,. \tag{II.4}$$

Work over graphic for mexican hat potential

Figure II.1a shows the free energy as a function of a single-component, real order parameter Ψ and it illustrates the essence of Landau theory: there are

two cases for the minima of the free energy F

$$\Psi = \begin{cases} 0 & T \geq T_C \\ \pm\sqrt{\frac{a(T_C - T)}{u}} & T < T_C \end{cases}, \tag{II.5}$$

so there is a for $T < T_C$ there are two minima corresponding to ground states with broken symmetry. When the order parameter can be calculated from some microscopic theory, the critical temperature T_C can be extracted from the behavior of the order parameter near T_C via a linear fit of

$$|\Psi|^2 \propto T_C - T \,. \tag{II.6}$$

Generalizing this from a one to an n-component order parameters is straightforward. One example is the complex or two component order parameter that will become important for

$$\Psi = \Psi_1 + \mathrm{i}\Psi_2 = |\Psi| e^{\mathrm{i}\phi} \,. \tag{II.7}$$

The Landau free energy then takes the form

$$F[\Psi] = r\Psi^*\Psi + \frac{u}{2}(\Psi^*\Psi)^2 = r|\Psi|^2 + \frac{u}{2}|\Psi|^4 \tag{II.8}$$

with again

$$r = a(T_C - T) \,. \tag{II.9}$$

Instead of the two minima, the free energy here is rotational symmetry, because it is independent of the phase of the order parameter:

$$F[\Psi] = f[e^{\mathrm{i}a}\Psi] \,. \tag{II.10}$$

This gives the so called 'Mexican hat' potential shown in fig. II.1b. In this potential, the order parameter can be rotated continuously from one broken-symmetry state to another.

In 1950, Ginzburg and Landau published their theory of superconductivity based on Landaus theory of phase transitions [24]. Where Landau theory as described above has an uniform order parameters, Ginzburg-Landau theory accounts for it being inhomogeneous, so an order parameter with spatially varying amplitude or direction. This in turn leads to the order parameter

developing a fixed phase, which is the underlying mechanism of the superflow in superconductors.

Ginzburg-Landau theory can be developed for a general n-component order parameter, but in superfluids and superconductors the order parameter is complex, i.e. two-component. The Ginzburg-Landau free energy for a complex order parameter is

$$F_{\mathrm{GL}}[\Psi, \Delta\Psi] = s|\Delta\Psi|^2 + r|\Psi|^2 + \frac{u}{2}|\Psi|^4 \,, \tag{II.11}$$

where the gradient term $\Delta\Psi$ is added in comparison to Landau energy.

Work over paragraph

In GL theory, energy is sensitive to a twist of the phase. Substitute $\psi = |\psi|e^{i\phi}$ into GL free energy, gradient term is:

$$\Delta\psi = (\Delta|\psi| + i\Delta\phi|\psi|)e^{i\phi} \tag{II.12}$$

So:

$$f_{GL} = s|\psi|^2(\Delta\phi)^2 + \left[s(\Delta|\psi|)^2 + r|\psi|^2 + \frac{u}{2}|\psi|^4\right] \tag{II.13}$$

The second term describes energy cost of variations in the magnitude of the order parameter. The first term describes energy cost of variations in the phase of the order parameter. The dominating fluctuation is determined by the ratio of the factors s and r, which has the dimension Length^2, from which define the correlation length

$$\xi = \sqrt{\frac{s}{|r|}} = \xi_0 \left(1 - \frac{T}{T_C}\right)^{-\frac{1}{2}} \tag{II.14}$$

where $\xi_0 = \xi(T = 0) = \sqrt{\frac{s}{aT_C}}$ is the coherence length. Beyond this length scale: only phase fluctuations survive.

Explanation superfluid weight

II.1.3 Superconducting Length Scales

From [20].

Better introduction

In most materials: Cooper pairs do not carry finite center-of-mass momentum. In presence of e.g. external fields or magnetism: SC states with FMP might arise.

Theory/procedure in the paper: enforce FMP states via constraints on pair-center-of-mass momentum $\mathbf{q}$, access characteristic lenght scales ξ_0, λ_L through

analysis of the momentum and temperature-dependent OP. FF-type pairing with Cooper pairs carrying finite momentum:

$$\psi_{\mathbf{q}}(\mathbf{r}) = |\psi_{\mathbf{q}}|e^{i\mathbf{qr}} \tag{II.15}$$

Then the free energy density is

$$f_{GL}[\psi_{\mathbf{q}}] = \alpha|\psi_{\mathbf{q}}|^2 + \frac{b}{2}|\psi_{\mathbf{q}}|^4 + \frac{\hbar^2 q^2}{2m^*}|\psi_{\mathbf{q}}|^2 \tag{II.16}$$

Stationary point of the system:

$$\frac{\delta f_{GL}}{\delta \psi^*_{\mathbf{q}}} = 2\psi_{\mathbf{q}}\left[\alpha(1-\xi^2 q^2) + b|\psi_{\mathbf{q}}|^2\right] = 0 \tag{II.17}$$

which results in the $\mathbf{q}$-dependence of the OP

$$|\psi_{\mathbf{q}}|^2 = |\psi_0|^2(1-\xi(T)^2 q^2) \tag{II.18}$$

For some value, SC order breaks down, $\psi_{\mathbf{q}_c} = 0$, because the kinetic energy from phase modulation exceeds the gain in energy from pairing. In GL theory: $q_c = \xi(T)^{-1}$. The temperature dependence of the OP and extracted $\xi(T)$ gives access to the coherence length via

$$\xi(T) = \xi_0(1-\frac{T}{T_C})^{-\frac{1}{2}} \tag{II.19}$$

Depairing current from FMP

Full formula for supercurrent, with sum over orbitals

DS from FMP

Write more about the connection between all the things here

Make graphic for Landau OP and BCS OP with q

Better introduction

The Cooper pair [25, 26]

II.2 Bardeen-Coooper-Schrieffer Theory

It took nearly 50 years after the first discovery of superconductivity in mercury by Heike Kamerlingh Onnes in 1911 [2] for the first microscopic description of this phenomenon to be published in 1957 by John Bardeen, Leon Cooper and J. Robert Schrieffer [4]. This BCS (Bardeen-Cooper-Schrieffer) theory is one of the great successes in physics history.

The BCS description of superconductivity is based on the fact that the Fermi sea is unstable towards development of bound pairs under arbitrarily small attraction [27]. The origin of the attractive interaction $V_{\mathbf{k},\mathbf{k}'}$, which Bardeen, Cooper and Schrieffer identified as a retarded electron-phonon interaction [4].

There exist many textbooks tackling BCS theory from different angles, such as chapter 14 in refs. [15, 16]. This section gives an introduction to the relevant physics of BCS theory as originally proposed, then derives the

II.2.1 BCS Hamiltonian

Work over paragraph

BCS-Hamiltonian:

$$H_{\text{BCS}} = \sum_{\mathbf{k}\sigma} \epsilon_{\mathbf{k}\sigma} c^\dagger_{\mathbf{k}\sigma} c_{\mathbf{k}\sigma} + \sum_{\mathbf{k},\mathbf{k}'} V_{\mathbf{k},\mathbf{k}'} c^\dagger_{\mathbf{k}\uparrow} c^\dagger_{-\mathbf{k}\downarrow} c_{-\mathbf{k}'\downarrow} c_{\mathbf{k}'\uparrow} \tag{II.20}$$

This Hamiltonian can be solved exactly using a mean field approach, because it involves an interaction at zero momentum and thus infinite range. Order parameter in mean field BCS theory is the pairing amplitude

$$\Delta = -\frac{U}{N_{\mathbf{k}}} \sum_{\mathbf{k}} \langle c_{-\mathbf{k}\downarrow} c_{\mathbf{k}\uparrow} \rangle = -U \langle c_{-\mathbf{r}=0\downarrow} c_{\mathbf{r}=\mathbf{0}\uparrow} \rangle \simeq U\Psi \, . \tag{II.21}$$

More about mean field theory in section II.2.2

A finite Δ corresponds to the pairing introduced above: there is a finite expectation value for a coherent creation/annihilation of a pair of electrons with opposite momentum and spin. A finite Δ also introduces a band gap into the spectrum. BCS theory brings multiple aspects together: concept of paired electrons with the pairing amplitude being the order parameter in SC, an explanation for the attractive interaction overcoming Coulomb repulsion and a model Hamiltonian that very elegantly captures the essential physics.

It is very successful in two ways: on the one hand it could quantitatively predict effects in the SCs known at the time, for example the Hebel-Slichter peak that was measured in 1957 [28, 29] and the band gap measured by Giaever in 1960 [30]. On the other hand, it established electronic pairing as the microscopic mechanism behind SC, which holds still today even for high T_C/unconventional superconductors, so SCs that cannot be described by BCS theory [31].

Other pairing interactions can be taken, gives explanations for a lot of different SCs

II.2.2 Multiband BCS Mean Field Theory

The Hubbard model is the simplest model for interacting electron systems. It goes back to works by Hubbard [32], Kanamori [33] and Gutzweiler [34].

$$H_{\text{int}} = U \sum_i c^\dagger_{i,\uparrow} c^\dagger_{i,\downarrow} c_{i,\downarrow} c_{i,\uparrow} \tag{II.22}$$

where $U > 0$.

Besides
[35]

Some relevance of the repulsive Hubbard model

This simple Hubbard model can be extended in a multitude of ways to model a variety of physical system. In this work: extension to multiple orbitals (i.e. atoms in the unit cell for lattice systems) and an attractive interaction, i.e. a negative U. Physical motivation for taking a negative-U Hubbard model: electrons can experience a local attraction interaction, for example through electrons coupling with phononic degrees of freedom or with electronic excitations that can be described as bosons [36]. The form of the interaction term is then:

There are some more specific papers to the specific mechanisms (and also some more mechanism), could cite these here and say some more things

$$H_{\text{int}} = -\sum_{i,\alpha} U_\alpha c^\dagger_{i,\alpha,\uparrow} c^\dagger_{i,\alpha,\downarrow} c_{i,\alpha,\downarrow} c_{i,\alpha,\uparrow} \tag{II.23}$$

where α counts orbitals and the minus sign in front is taken so that $U > 0$ now corresponds to an attractive interaction (this is purely convention).

There are a multitude of ways to derive a mean field description of a given interacting Hamiltonian. Very rigorous in path integral formulations as saddle points, given for example in ref. [15]. The review follows [37]. A more intuitive way based on ref. [17] discussed here looks at the operators and which one are small.

Order of operators? -> also in all other equations!

Look at interaction term eq. (II.23). Mean-field approximation (here specifically for superconductivity i.e. pairing): operators do not deviate much from their average value, i.e. the deviation operators

there are other combinations, talk about that

deviations with small deltas

$$d_{i,\alpha} = c^\dagger_{i,\alpha,\uparrow} c^\dagger_{i,\alpha,\downarrow} - \langle c^\dagger_{i,\alpha,\uparrow} c^\dagger_{i,\alpha,\downarrow} \rangle \tag{II.24}$$

$$e_{i,\alpha} = c_{i,\alpha,\downarrow} c_{i,\alpha,\uparrow} - \langle c_{i,\alpha,\downarrow} c_{i,\alpha,\uparrow} \rangle \tag{II.25}$$

are small (dont contribute much to expectation values and correlation functions), so that in the interaction part of the Hamiltonian

$$\begin{aligned}
H_{\text{int}} &= -\sum_{i,\alpha} U_\alpha c^\dagger_{i,\alpha,\uparrow} c^\dagger_{i,\alpha,\downarrow} c_{i,\alpha,\downarrow} c_{i,\alpha,\uparrow} && \text{(II.26)}\\
&= -\sum_{i,\alpha} U_\alpha \left(d^\dagger_{i,\alpha} + \langle c^\dagger_{i,\alpha,\uparrow} c^\dagger_{i,\alpha,\downarrow} \rangle \right) \left(e_{i,\alpha} + \langle c_{i,\alpha,\downarrow} c_{i,\alpha,\uparrow} \rangle \right) && \text{(II.27)}\\
&= -\sum_{i,\alpha} U_\alpha (d_{i,\alpha} e_{i,\alpha} + d_{i,\alpha} \langle c_{i,\alpha,\downarrow} c_{i,\alpha,\uparrow} \rangle + e_{i,\alpha} \langle c^\dagger_{i,\alpha,\uparrow} c^\dagger_{i,\alpha,\downarrow} \rangle && \text{(II.28)}\\
&\quad + \langle c^\dagger_{i,\alpha,\uparrow} c^\dagger_{i,\alpha,\downarrow} \rangle \langle c_{i,\alpha,\downarrow} c_{i,\alpha,\uparrow} \rangle) && \text{(II.29)}
\end{aligned}$$

the first term is quadratic in the deviation and can be neglected. Thus arrive at the approximation

$$H_{\text{int}} \approx -\sum_{i,\alpha} U_\alpha \left(d_{i,\alpha} \langle c_{i,\alpha,\downarrow} c_{i,\alpha,\uparrow} \rangle + e_{i,\alpha} \langle c^\dagger_{i,\alpha,\uparrow} c^\dagger_{i,\alpha,\downarrow} \rangle + \langle c^\dagger_{i,\alpha,\uparrow} c^\dagger_{i,\alpha,\downarrow} \rangle \langle c_{i,\alpha,\downarrow} c_{i,\alpha,\uparrow} \rangle \right) \tag{II.30}$$

$$= -\sum_{i,\alpha} U_\alpha (c^\dagger_{i,\alpha,\uparrow} c^\dagger_{i,\alpha,\downarrow} \langle c_{i,\alpha,\downarrow} c_{i,\alpha,\uparrow} \rangle + c_{i,\alpha,\downarrow} c_{i,\alpha,\uparrow} \langle c^\dagger_{i,\alpha,\uparrow} c^\dagger_{i,\alpha,\downarrow} \rangle \tag{II.31}$$

$$- \langle c^\dagger_{i,\alpha,\uparrow} c^\dagger_{i,\alpha,\downarrow} \rangle \langle c_{i,\alpha,\downarrow} c_{i,\alpha,\uparrow} \rangle) \tag{II.32}$$

$$= \sum_{i,\alpha} (\Delta_{i,\alpha} c^\dagger_{i,\alpha,\uparrow} c^\dagger_{i,\alpha,\downarrow} + \Delta^*_{i,\alpha} c_{i,\alpha,\downarrow} c_{i,\alpha,\uparrow} - \frac{|\Delta_{i,\alpha}|^2}{U_\alpha}) \tag{II.33}$$

with the expectation value

$$\Delta_{i,\alpha} = -U_\alpha \langle c_{i,\alpha,\downarrow} c_{i,\alpha,\uparrow} \rangle \tag{II.34}$$

which is called the superconducting gap. Using the Fourier transform

$$c_{i\alpha\sigma} = \frac{1}{\sqrt{N}} \sum_{\mathbf{k}} e^{i\mathbf{k}\mathbf{r}_{i\alpha}} c_{\mathbf{k}\alpha\sigma} \tag{II.35}$$

can write

$$H_{\text{MF}} = \sum_{\mathbf{k}\alpha\beta\sigma} [H_{0,\sigma}(\mathbf{k})]_{\alpha\beta} c^\dagger_{\mathbf{k}\alpha\sigma} c_{\mathbf{k}\beta\sigma} - \mu \sum_{\mathbf{k}\alpha\sigma} n_{\mathbf{k}\alpha\sigma} + \sum_{\alpha,\mathbf{k}} (\Delta_\alpha c^\dagger_{\mathbf{k}\alpha\uparrow} c^\dagger_{-\mathbf{k}\alpha\downarrow} + \Delta^*_\alpha c_{-\mathbf{k}\alpha\downarrow} c_{\mathbf{k}\alpha\uparrow}) \tag{II.36}$$

Look at that Hamiltonian again, is that correct and can I write it better?

To include finite momentum, take the ansatz of a Fulde-Ferrel (FF) type pairing [38]:

$$\Delta \tag{II.37}$$

How to include finite momentum, rewrite equations

The Hamiltonian in eq. (II.36) can be writen as

$$H_{\text{MF}} = \sum_{\mathbf{k}} \mathbf{C}^\dagger_{\mathbf{k}} H_{\text{BdG}}(\mathbf{k}) \mathbf{C}_{\mathbf{k}} \tag{II.38}$$

Get the remaining terms here

$$C_{\mathbf{k}} = \begin{pmatrix} c_{\mathbf{k}1\uparrow} & c_{\mathbf{k}2\uparrow} & \cdots & c_{\mathbf{k}n_{\text{orb}}\uparrow} & c^\dagger_{-\mathbf{k}1\downarrow} & c^\dagger_{-\mathbf{k}2\downarrow} & \cdots & c^\dagger_{-\mathbf{k}n_{\text{orb}}\downarrow} \end{pmatrix}^T \tag{II.39}$$

with the so-called Bogoliubov-de-Gennes matrix

$$H_{\text{BdG}}(\mathbf{k}) = \begin{pmatrix} H_{0,\uparrow}(\mathbf{k}) - \mu & \Delta \\ \Delta^\dagger & -H^*_{0,\downarrow}(-\mathbf{k}) + \mu \end{pmatrix} \tag{II.40}$$

with $H_{0,\sigma}$ being the F.T. of the kinetic term and $\Delta = \mathrm{diag}(\Delta_1, \Delta_2, \dots, \Delta_{n_{\mathrm{orb}}})$.

Formula for OP using the Bogoliubov operators

$$\Delta_\alpha = -U \tag{II.41}$$

II.3 Dynamical Mean-Field Theory (DMFT)

II.3.1 Green's Function Formalism

Green's functions: method to encode influence of many-body effects on propagation of particles in a system.

Following [17]

Have different kinds of Green's functions, for example the retarded Green's function (here with the k for lattice systems):

$$G^R(\mathbf{k}, \sigma, \sigma' t) = -\mathrm{i}\Theta(t - t') \langle\{c_{\mathbf{k}\sigma}(t), c^\dagger_{\mathbf{k}\sigma'}(0)\}\rangle \tag{II.42}$$

They give the amplitude of a particle inserted at momentum $\mathbf{k}'$ at time t' to propagate to position $\mathbf{k}$ at time t. Define Fourier-transform:

$$G^R(\mathbf{k}, \sigma, \sigma', \omega) = \int_{-\infty}^{\infty} \mathrm{d}t G^R(\mathbf{k}, \sigma, \sigma' t) \tag{II.43}$$

Can define the spectral function from this:

$$A(\mathbf{k}\sigma, \omega) = -2\Im G^R(\mathbf{k}\sigma, \omega) \tag{II.44}$$

Looking at the diagonal elements of G^R here. The spectral function can be thought of as the energy resolution of a particle with energy ω. This mean, for non-interacting systems, the spectral function is a delta-function around the single-particle energies:

$$A_0(\mathbf{k}\sigma, \omega) = 2\pi\delta(\omega - \epsilon_{\mathbf{k}\sigma}) \tag{II.45}$$

For interacting systems this is not true, but A can still be peaked.

A mathematical trick to calculate GFs in praxis is to introduce the imaginary time variable τ

$$t \to -\mathrm{i}\tau \tag{II.46}$$

General mu mean field theory

Write indec erywhere w comma

How to solve mean field theory self-consistently

SC current in BCS

Introduction DMFT, citing what has been achieved with it so far, what is the basic idea etc.

Give an introduction

Work over the paragraph

Slim down to relevant information

Show GFs can be related to observables

where τ is real and has the dimension time. This enables the simultaneous expansion of exponential $e^{-\beta H}$ coming from the thermodynamic average and $e^{-\mathrm{i}Ht}$ coming from the time evolution of operators. Define Matsubara GF $C_{AB}(\tau, 0)$:

e Greens instead of n functions

$$C_{AB}(\tau, 0) = -\langle T_\tau(A(\tau)B(0))\rangle \tag{II.47}$$

with time-ordering operator in imaginary time:

$$T_\tau(A(\tau)B(\tau')) = \Theta(\tau - \tau')A(\tau)B(\tau') \pm \Theta(\tau' - \tau)B(\tau')A(\tau) \tag{II.48}$$

so that operators with later 'times' go to the left.

Can prove from properties of Matsubara GF, that they are only defined for

$$-\beta < \tau < \beta \tag{II.49}$$

Due to this, the Fourier transform of the Matsubara GF is defined on discrete values:

$$C_{AB}(\mathrm{i}\omega_n) = \int_0^\beta \mathrm{d}\tau \tag{II.50}$$

with fermionic/bosonic Matsubara frequencies

$$\omega_n = \begin{cases} \frac{2n\pi}{\beta} \text{ for bosons} \\ \frac{(2n+1)\pi}{\beta} \text{ for fermions} \end{cases} \tag{II.51}$$

It turns out that Matsubara GFs and retarded GFs can be generated from a common function $C_{AB}(z)$ that is defined on the entire complex plane except for the real axis. So we can get the retarded GF $C^R_{AB}(\omega)$ by analytic continuation:

$$C^R_{AB}(\omega) = C_{AB}(\mathrm{i}\omega_n \to \omega + \mathrm{i}\eta) \tag{II.52}$$

So in particular the extrapolation of the Matsubara GF to zero is proportional to the density of states at the chemical potential. Gapped: density is zero (Matsubara GF goes to 0), metal: density is finite (Matsubara GF goes to finite value).

What is the eta there -> need to define it in retarded GF

single-particle Matsubara GF

II.3.2 Self Energy

Short introduction to diagrams

Dyson equation:

$$\mathcal{G}_\sigma(\mathbf{k}, \mathrm{i}\omega_n) = \frac{\mathcal{G}^0_\sigma(\mathbf{k}, \mathrm{i}\omega_n)}{1 - \mathcal{G}^0_\sigma(\mathbf{k}, \mathrm{i}\omega_n)\Sigma_\sigma(\mathbf{k}, \mathrm{i}\omega_n)} = \frac{1}{\mathrm{i}\omega_n - \xi_{\mathbf{k}-\Sigma_\sigma(\mathbf{k}, \mathrm{i}\omega_n)}} \tag{II.53}$$

Self energy

Dyson equation

II.3.3 Nambu-Gorkov GF

More general introduction into NG GFs, how they look like, what they describe etc.

Introduction following [15, ch. 14.7]

Order parameter can be chosen as the anomalous GF:

$$\Psi = F^{\mathrm{loc}}(\tau = 0^-) \tag{II.54}$$

or the superconducting gap

$$\Delta = Z\Sigma^{\mathrm{AN}} \tag{II.55}$$

that can be calculated from the anomalous self-energy Σ^{AN} and quasiparticle weight Z

Sources for these?

How to get quasiparticle weight?

II.3.4 DMFT

Following [39].

Most general non-interacting electronic Hamiltonian in second quantization:

$$H_0 = \sum_{i,j,\sigma} \tag{II.56}$$

with lattice coordinates i, j and spin σ.

One particle Green's function (many-body object, coming from the Hubbard model):

$$G(\mathbf{k}, \mathrm{i}\omega_n) = \frac{1}{\mathrm{i}\omega_n + \mu - \epsilon_{\mathbf{k}} - \Sigma(\mathbf{k}, \mathrm{i}\omega_n)} \tag{II.57}$$

with the self energy $\Sigma(\mathrm{i}\omega_n)$ coming from the solution of the effect on-site problem:

The Dyson equation

$$G(\mathbf{k}, \mathrm{i}\omega_n) = \left(G_0(\mathbf{k}, \mathrm{i}\omega_n) - \Sigma(\mathbf{k}, \mathrm{i}\omega_n)\right)^{-1} \tag{II.58}$$

relates the non-interacting Greens function $G_0(\mathbf{k}, \mathrm{i}\omega_n)$ and the fully-interacting Greens function $G(\mathbf{k}, \mathrm{i}\omega_n)$ (inversion of a matrix!).

III Dressed Graphene Model

Write introduction to the model and what is done in this chapter

III.1 Lattice Structure

Structure of honeycomb lattice following [40].

Monolayer graphene forms a honeycomb lattice, which is a hexagonal Bravais lattice with a two atom basis.

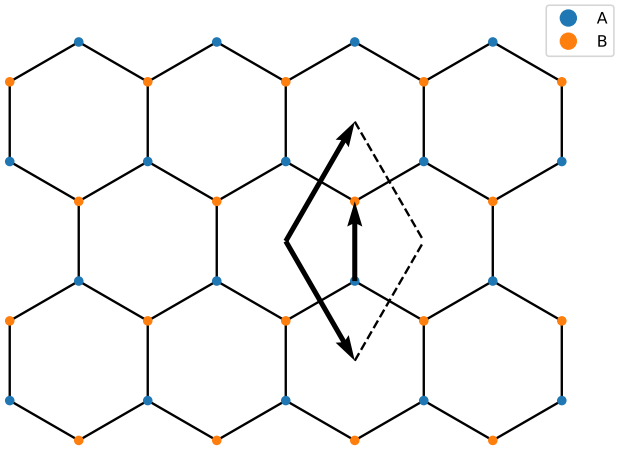

Figure III.1: *Graphene lattice structure*

Primitive lattice vectors of the hexagonal lattice:

$$\mathbf{a}_1 = \frac{a}{2}\begin{pmatrix} 1 \\ \sqrt{3} \end{pmatrix} \tag{III.1}$$

$$\mathbf{a}_2 = \frac{a}{2}\begin{pmatrix} 1 \\ -\sqrt{3} \end{pmatrix} \tag{III.2}$$

with lattice constant $a \approx 2.46$ Å (distance between unit cells). Have

$$a = \sqrt{3}a_0 \tag{III.3}$$

with the nearest-neighbour distance a_0.

Vectors to the nearest-neighbor B_i $(i = 1, 2, 3,)$ atoms from atom A:

$$\delta_{AB,1} = \begin{pmatrix} 0 \\ \frac{a}{\sqrt{3}} \end{pmatrix}, \delta_{AB,2} = \begin{pmatrix} \frac{a}{2} \\ -\frac{a}{2\sqrt{3}} \end{pmatrix}, \delta_{AB,3} = \begin{pmatrix} -\frac{a}{2} \\ -\frac{a}{2\sqrt{3}} \end{pmatrix} \tag{III.4}$$

Vectors to the nearest-neighbor A_i $(i = 1, 2, 3,)$ atoms from atom B:

$$\delta_{BA,1} = \begin{pmatrix} 0 \\ -\frac{a}{\sqrt{3}} \end{pmatrix}, \delta_{BA,2} = \begin{pmatrix} \frac{a}{2} \\ \frac{a}{2\sqrt{3}} \end{pmatrix}, \delta_{BA,3} = \begin{pmatrix} -\frac{a}{2} \\ \frac{a}{2\sqrt{3}} \end{pmatrix} \tag{III.5}$$

The vectors between the Graphene A atom and the six neighbours on the same sub lattice can be found by rotating $\mathbf{a}_1$ six times by $1/6 * 2\pi = \pi/3$:

$$\delta_{AA,1} = \mathbf{a}_1 = \frac{a}{2}\begin{pmatrix} 1 \\ \sqrt{3} \end{pmatrix} = a\begin{pmatrix} \frac{1}{2} \\ \frac{\sqrt{3}}{2} \end{pmatrix} = a\begin{pmatrix} \sin(\frac{\pi}{6}) \\ \cos(\frac{\pi}{6}) \end{pmatrix} \tag{III.6}$$

$$\delta_{AA,2} = a\begin{pmatrix} \sin(\frac{3\pi}{6}) \\ \cos(\frac{3\pi}{6}) \end{pmatrix} = a\begin{pmatrix} 1 \\ 0 \end{pmatrix} \tag{III.7}$$

$$\delta_{AA,3} = a\begin{pmatrix} \sin(\frac{5\pi}{6}) \\ \cos(\frac{5\pi}{6}) \end{pmatrix} = a\begin{pmatrix} \frac{1}{2} \\ -\frac{\sqrt{3}}{2} \end{pmatrix} \tag{III.8}$$

$$\delta_{AA,4} = a\begin{pmatrix} \sin(\frac{7\pi}{6}) \\ \cos(\frac{7\pi}{6}) \end{pmatrix} = a\begin{pmatrix} -\frac{1}{2} \\ -\frac{\sqrt{3}}{2} \end{pmatrix} \tag{III.9}$$

$$\delta_{AA,5} = a\begin{pmatrix} \sin(\frac{9\pi}{6}) \\ \cos(\frac{9\pi}{6}) \end{pmatrix} = a\begin{pmatrix} -1 \\ 0 \end{pmatrix} \tag{III.10}$$

$$\delta_{AA,6} = a\begin{pmatrix} \sin(\frac{11\pi}{6}) \\ \cos(\frac{11\pi}{6}) \end{pmatrix} = a\begin{pmatrix} -\frac{1}{2} \\ \frac{\sqrt{3}}{2} \end{pmatrix} \tag{III.11}$$

First BZ vs this Gamma centered one

The primitive reciprocal lattice vectors $\mathbf{b}_1$, $\mathbf{b}_2$ fulfill

$$\mathbf{a}_1 \cdot \mathbf{b}_1 = \mathbf{a}_2 \cdot \mathbf{b}_2 = 2\pi \tag{III.12}$$

$$\mathbf{a}_1 \cdot \mathbf{b}_2 = \mathbf{a}_2 \cdot \mathbf{b}_1 = 0\,, \tag{III.13}$$

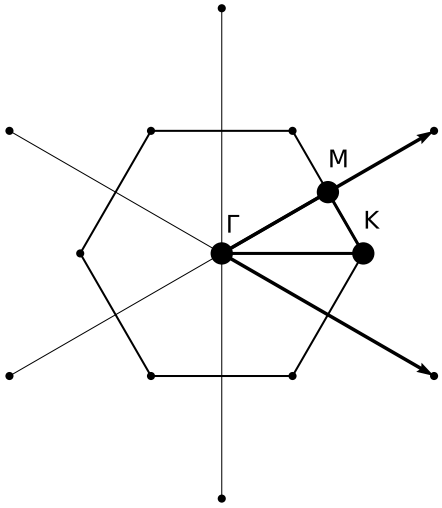

Figure III.2: *Graphene Brillouin Zone*

so we have:

$$\mathbf{b}_1 = \frac{2\pi}{a}\begin{pmatrix} 1 \\ \frac{1}{\sqrt{3}} \end{pmatrix} \tag{III.14}$$

$$\mathbf{b}_2 = \frac{2\pi}{a}\begin{pmatrix} 1 \\ -\frac{1}{\sqrt{3}} \end{pmatrix} \tag{III.15}$$

Points of high symmetry in the Brillouin zone are:

$$\Gamma = \begin{pmatrix} 0 \\ 0 \end{pmatrix} \tag{III.16}$$

$$\mathrm{M} = \frac{\pi}{a}\begin{pmatrix} 1 \\ \frac{1}{\sqrt{3}} \end{pmatrix} \tag{III.17}$$

$$\mathrm{K} = \frac{4\pi}{3a}\begin{pmatrix} 1 \\ 0 \end{pmatrix} \tag{III.18}$$

III.2 Dressed Graphene Model

Graphene lattice and a site X.

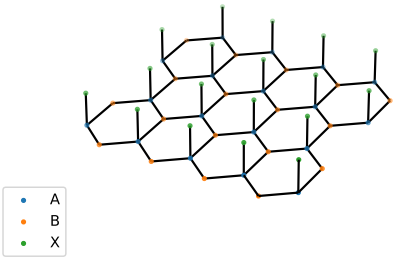

Figure III.3: *EG-X model*

Without interaction:

$$H_0 = -t_X \sum_{\langle ij\rangle,\sigma} d^\dagger_{i,\sigma} d_{j,\sigma} - t_{\mathrm{Gr}} \sum_{\langle ij\rangle,\sigma} c^{(A),\dagger}_{i,\sigma} c^{(B)}_{j,\sigma} + V \sum_{i,\sigma\sigma'} d^\dagger_{i,\sigma} c^{(A)}_{i,\sigma'} + \text{h.c.} \tag{III.19}$$

with:

- d operators on the X atom
- $c^{(\epsilon)}$ operators on the graphene site ($\epsilon = A, B$)
- t_X NN hopping for X
- t_{Gr} NN hopping of Gr
- V hybridization between X and Graphene B sites

We can also introduce an onsite Hubbard interaction:

$$H_{\mathrm{int}} = U_X \sum_i d^\dagger_{i,\uparrow} d^\dagger_{i,\downarrow} d_{i,\downarrow} d_{i,\uparrow} + U_{\mathrm{Gr}} \sum_{i,\epsilon=A,B} c^{(\epsilon)\dagger}_{i,\uparrow} c^{(\epsilon)\dagger}_{i,\downarrow} c^{\epsilon}_{i,\downarrow} c^{\epsilon}_{i,\uparrow} \tag{III.20}$$

Hamilto-
n orbital

Define sublattice index

$$\alpha = 1, 2, 3 \tag{III.21}$$

with $1 \mathrel{\widehat{=}} \mathrm{Gr}_1, 2 \mathrel{\widehat{=}} \mathrm{Gr}_2, 3 \mathrel{\widehat{=}} \mathrm{X}$. Then we can write the non-interacting term as

$$H_0 = -\sum_{\langle i,j\rangle,\alpha,\beta,\sigma} [\mathbf{t}]_{i\alpha,j\beta}\, c^\dagger_{i\alpha} c_{j\beta} \tag{III.22}$$

with the matrix

$$\mathbf{t} = \begin{pmatrix} 0 & t_{\mathrm{Gr}} & 0 \\ t_{\mathrm{Gr}} & 0 & -V\delta_{ij} \\ 0 & -V\delta_{ij} & t_{\mathrm{X}} \end{pmatrix} \tag{III.23}$$

Add chemical potential:

$$-\mu \sum_{i\alpha\sigma} n_{i\alpha\sigma} \tag{III.24}$$

Also write the interaction part with α (with changed signs compared to Niklas, to keep in line with papers about the attractive Hubbard model):

$$H_{int} = -\sum_{i\alpha} U_\alpha c^\dagger_{i\alpha\uparrow} c^\dagger_{i\alpha\downarrow} c_{i\alpha\downarrow} c_{i\alpha\uparrow} \tag{III.25}$$

$$H_0 = \sum_{\mathbf{k},\sigma,\sigma'} \begin{pmatrix} c^{A,\dagger}_{k,\sigma} & c^{B,\dagger}_{k,\sigma} & d^\dagger_{k,\sigma} \end{pmatrix} \begin{pmatrix} 0 & f_{Gr} & V \\ f^*_{Gr} & 0 & 0 \\ V & 0 & f_{\mathrm{X}} \end{pmatrix} \begin{pmatrix} c^A_{k,\sigma} \\ c^B_{k,\sigma} \\ d_{k,\sigma} \end{pmatrix} \tag{III.26}$$

The band structure for the non-interacting EG-X model is easily obtained by diagonalising the matrix in eq. (III.26). This was done in fig. III.4.

Values used for calculation:

- $a_0 = 1$
- $t_{\mathrm{Gr}} = 1$
- $t_{\mathrm{X}} = 0.01$

V is the control parameter. A range from $V = 0.1$ to $V = 2$ can be mapped onto materials in experiment.

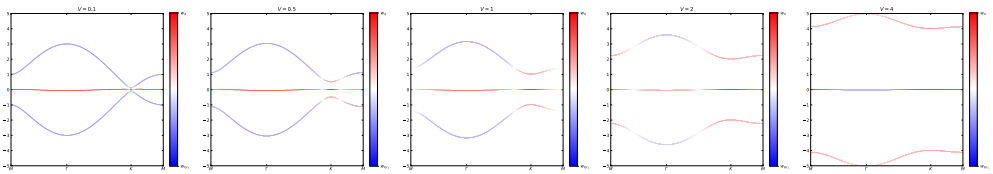

Figure III.4: *Bands of the non-interacting EG-X model. All the bands are spin-degenerate.*

IV Results

Parameter sweeps using [41].

IV.1 Gaps

IV.2 Superfluid Weight

IV.3 Breakdown of SC with finite momentum

IV.4 Coherence length etc.

Explain how to get the length scales in the different ways

Specifically: take

$$\xi(T) = \frac{1}{\sqrt{2}|\mathbf{Q}|} \tag{IV.1}$$

with $\mathbf{Q}$ such that

$$|\frac{\psi_{\mathbf{Q}}(T)}{\psi_0(T)}| = \frac{1}{\sqrt{2}} \tag{IV.2}$$

A Dressed Graphene Hamiltonian in Reciprocal Space

Clean up this section

In this chapter, the model Hamiltonian from section III.2

$$H_0 = -t_X \sum_{\langle ij\rangle,\sigma} d^\dagger_{i,\sigma} d_{j,\sigma} - t_{Gr} \sum_{\langle ij\rangle,\sigma} c^{(A),\dagger}_{i,\sigma} c^{(B)}_{j,\sigma} + V \sum_{i,\sigma} d^\dagger_{i,\sigma} c^{(A)}_{i,\sigma} + \text{h.c.} \tag{A.1}$$

will be treated to obtain the electronic band structure. The first step is to write out the sums over nearest neighbors $\langle i,j\rangle$ explicitly, writing $\delta_X, \delta_\epsilon$ ($\epsilon = A, B$) for the vectors to the nearest neighbors of the X atoms and Graphene A, B sites. Doing the calculation for example of the X atoms:

$$-t_X \sum_{\langle ij\rangle,\sigma} (d^\dagger_{i,\sigma} d_{j,\sigma} + d^\dagger_{j,\sigma} d_{i,\sigma}) = -\frac{t_X}{2} \sum_{i,\sigma} \sum_{\delta_X} d^\dagger_{i,\sigma} d_{i+\delta_X,\sigma} - \frac{t_X}{2} \sum_{j,\sigma} \sum_{\delta_X} d^\dagger_{j,\sigma} d_{j+\delta_X,\sigma} \tag{A.2}$$

$$= -t_X \sum_{i,\sigma} \sum_{\delta_X} d^\dagger_{i,\sigma} d_{i+\delta_X,\sigma} \tag{A.3}$$

The factor $1/2$ in eq. (A.2) is to account for double counting when going to the sum over all lattice sites i. By relabeling $j \to i$ in the second sum, the two sum are the same and eq. (A.3) is obtained. Using now the discrete Fourier transform

$$c_i = \frac{1}{\sqrt{N}} \sum_{\mathbf{k}} e^{i\mathbf{k}\mathbf{r}_i} c_{\mathbf{k}}, \; c^\dagger_i = \frac{1}{\sqrt{N}} \sum_{\mathbf{k}} e^{-i\mathbf{k}\mathbf{r}_i} c^\dagger_{\mathbf{k}} \tag{A.4}$$

with the completeness relation

$$\sum_i e^{i\mathbf{k}\mathbf{r}_i} e^{-i\mathbf{k}'\mathbf{r}_i} = N \delta_{\mathbf{k},\mathbf{k}'} \,, \tag{A.5}$$

eq. (A.3) reads:

$$-t_X \frac{1}{N} \sum_{i,\sigma} \sum_{\delta_X} d^\dagger_{i,\sigma} d_{i+\delta_X,\sigma} = -t_X \frac{1}{N} \sum_{i,\sigma} \sum_{\mathbf{k},\mathbf{k}',\delta_X} \left(e^{-i\mathbf{k}\mathbf{r}_i} d^\dagger_{\mathbf{k},\sigma} \right) \left(e^{i\mathbf{k}'\mathbf{r}_i} e^{i\mathbf{k}'\delta_X} d_{\mathbf{k}',\sigma} \right) \tag{A.6}$$

$$= -t_X \frac{1}{N} \sum_{\mathbf{k},\mathbf{k}',\delta_X,\sigma} d^\dagger_{\mathbf{k},\sigma} d_{\mathbf{k}',\sigma} e^{i\mathbf{k}'\delta_X} \sum_i e^{-i\mathbf{k}\mathbf{r}_i} e^{i\mathbf{k}'\mathbf{r}_i} \tag{A.7}$$

$$= -t_X \frac{1}{N} \sum_{\mathbf{k},\mathbf{k}',\sigma} d^\dagger_{\mathbf{k},\sigma} d_{\mathbf{k}',\sigma} \sum_{\delta_X} e^{i\mathbf{k}'\delta_X} \left(N \delta_{\mathbf{k},\mathbf{k}'} \right) \tag{A.8}$$

$$= -t_X \sum_{\mathbf{k},\sigma} d^\dagger_{\mathbf{k},\sigma} d_{\mathbf{k},\sigma} \sum_{\delta_X} e^{i\mathbf{k}\delta_X} \, . \tag{A.9}$$

This part is now diagonal in $\mathbf{k}$ space. The nearest neighbours vectors δ_X for the X atoms are the vectors $\delta_{AA,i}$ from section III.1. With that, the sum over δ_X can be explicitly calculated:

Correct exp expressions

Example for a vector product

$$f_X(\mathbf{k}) = -t_X \sum_{\delta_X} e^{i\mathbf{k}\delta_X} \tag{A.10}$$

$$= -t_X \left[\exp\left(ia \left(\frac{k_x}{2} + \frac{\sqrt{3}k_y}{2} \right) \right) + e^{iak_x} + e^{ia(\frac{k_x}{2} - \frac{\sqrt{3}k_y}{2})} \right. \tag{A.11}$$

$$\left. + \, e^{ia(-\frac{k_x}{2} - \frac{\sqrt{3}k_y}{2})} + e^{-iak_x} + e^{ia(-\frac{k_x}{2} + \frac{\sqrt{3}k_y}{2})} \right] \tag{A.12}$$

$$= -t_X \left(2\cos(ak_x) + 2e^{ia\frac{\sqrt{3}k_y}{2}} \cos\left(\frac{a}{2}k_x\right) + 2e^{-ia\frac{\sqrt{3}k_y}{2}} \cos\left(\frac{a}{2}k_x\right) \right) \tag{A.13}$$

$$= -2t_X \left(\cos(ak_x) + 2\cos\left(\frac{a}{2}k_x\right) \cos\left(\sqrt{3}\frac{a}{2}k_y\right) \right) \, . \tag{A.14}$$

The same can be done for the hopping between Graphene sites, for example :

$$-t_{\mathrm{Gr}} \sum_{\langle ij \rangle,\sigma\sigma'} c^{(A),\dagger}_{i,\sigma} c^{(B)}_{j,\sigma'} = -t_{\mathrm{Gr}} \sum_{i,\sigma\sigma'} \sum_{\delta_{AB}} c^{(A),\dagger}_{i,\sigma} c^{(B)}_{i+\delta_{AB},\sigma'} \tag{A.15}$$

$$= -t_{\mathrm{Gr}} \sum_{\mathbf{k},\sigma,\sigma'} c^{(A)\dagger}_{\mathbf{k},\sigma} c^{(B)}_{\mathbf{k},\sigma'} \sum_{\delta_{AB}} e^{i\mathbf{k}\delta_{AB}} \tag{A.16}$$

Show that!

We note

$$\sum_{\delta_{AB}} e^{i\mathbf{k}\delta_{AB}} = \left(\sum_{\delta_{BA}} e^{i\mathbf{k}\delta_{BA}} \right)^* = \sum_{\delta_{BA}} e^{-i\mathbf{k}\delta_{BA}} \tag{A.17}$$

and calculate

$$f_{Gr} = -t_{Gr} \sum_{\delta_{AB}} e^{\mathrm{i}\mathbf{k}\boldsymbol{\delta}_{AB}} \tag{A.18}$$

$$= -t_{Gr} \left(e^{\mathrm{i}\frac{a}{\sqrt{3}}k_y} + e^{\mathrm{i}\frac{a}{2\sqrt{3}}(\sqrt{3}k_x - k_y)} + e^{\mathrm{i}\frac{a}{2\sqrt{3}}(-\sqrt{3}k_x - k_y)} \right) \tag{A.19}$$

$$= -t_{Gr} \left(e^{\mathrm{i}\frac{a}{\sqrt{3}}k_y} + e^{-\mathrm{i}\frac{a}{2\sqrt{3}}k_y} \left(e^{\mathrm{i}\frac{a}{2}k_x} + e^{-\mathrm{i}\frac{a}{2}k_x} \right) \right) \tag{A.20}$$

$$= -t_{Gr} \left(e^{\mathrm{i}\frac{a}{\sqrt{3}}k_y} + 2e^{-\mathrm{i}\frac{a}{2\sqrt{3}}k_y} \cos\left(\frac{a}{2}k_x\right) \right) \tag{A.21}$$

All together, we get:

$$H_0 = \sum_{\mathbf{k},\sigma,\sigma'} \begin{pmatrix} c^{A,\dagger}_{k,\sigma} & c^{B,\dagger}_{k,\sigma} & d^{\dagger}_{k,\sigma} \end{pmatrix} \begin{pmatrix} 0 & f_{Gr} & V \\ f^*_{Gr} & 0 & 0 \\ V & 0 & f_X \end{pmatrix} \begin{pmatrix} c^{A}_{k,\sigma} \\ c^{B}_{k,\sigma} \\ d_{k,\sigma} \end{pmatrix} \tag{A.22}$$

B Notes on the Computational Implementation

All the code is available at github.com/Ruberhauptmann/quant-met.

All the data,

Data availability

For reproducibility, Datalad [42] is used.

The implementation relies on the work of many contributors of packages in Pythons ecosystem, most important among them NumPy [43], SciPy [44], Matplotlib [45], Pandas [46, 47] and Parasweep [41].

What software for what?

Bibliography

[1] U. of Chicago. *Annual Register*. 1893-1930. 462 pp. (cit. on p. 1).

[2] H. K. Onnes. "Further Experiments with Liquid Helium. G. On the Electrical Resistance of Pure Metals, Etc. VI. On the Sudden Change in the Rate at Which the Resistance of Mercury Disappears." In: *Through Measurement to Knowledge: The Selected Papers of Heike Kamerlingh Onnes 1853–1926*. Ed. by K. Gavroglu and Y. Goudaroulis. Dordrecht: Springer Netherlands, pp. 267–272. ISBN: 978-94-009-2079-8. DOI: 10.1007/978-94-009-2079-8_17 (cit. on pp. 1, 8).

[3] W. Meissner and R. Ochsenfeld. "Ein neuer Effekt bei Eintritt der Supraleitfähigkeit". In: *Naturwissenschaften* 21.44 (), pp. 787–788. ISSN: 1432-1904. DOI: 10.1007/BF01504252 (cit. on p. 1).

[4] J. Bardeen, L. N. Cooper, and J. R. Schrieffer. "Theory of Superconductivity". In: *Physical Review* 108.5 (), pp. 1175–1204. DOI: 10.1103/PhysRev.108.1175 (cit. on pp. 1, 8).

[5] J. G. Bednorz and K. A. Müller. "Possible High Tc Superconductivity in the Ba−La−Cu−O System". In: *Zeitschrift für Physik B Condensed Matter* 64.2 (), pp. 189–193. ISSN: 1431-584X. DOI: 10.1007/BF01303701 (cit. on p. 1).

[6] S.-i. Uchida et al. "High Tc Superconductivity of La-Ba-Cu Oxides". In: *Japanese Journal of Applied Physics* 26 (1A), p. L1. ISSN: 1347-4065. DOI: 10.1143/JJAP.26.L1 (cit. on p. 1).

[7] D. Rybicki et al. "Perspective on the Phase Diagram of Cuprate High-Temperature Superconductors". In: *Nature Communications* 7.1 (), p. 11413. ISSN: 2041-1723. DOI: 10.1038/ncomms11413 (cit. on p. 1).

[8] P. A. Rinck. *Magnetic Resonance in Medicine - A Critical Introduction*. ISBN: 978-628-01-2260-1. URL: http://www.magnetic-resonance.org/ (cit. on p. 1).

[9] A. Tollestrup and E. Todesco. "The Development of Superconducting Magnets for Use in Particle Accelerators: From the Tevatron to the LHC". In: *Reviews of Accelerator Science and Technology* 1.01 (), pp. 185–210 (cit. on p. 1).

[10] K. Irwin and G. Hilton. "Transition-Edge Sensors". In: *Cryogenic Particle Detection*. Ed. by C. Enss. Berlin, Heidelberg: Springer, pp. 63–150. ISBN: 978-3-540-31478-3. DOI: 10.1007/10933596_3 (cit. on p. 1).

[11] M. I. Faley et al. "High-Tc SQUID Biomagnetometers". In: *Superconductor Science and Technology* 30.8 (), p. 083001. ISSN: 0953-2048. DOI: 10.1088/1361-6668/aa73ad (cit. on p. 1).

[12] A. M. Klushin et al. "Present and Future of High-Temperature Superconductor Quantum-Based Voltage Standards". In: *IEEE Instrumentation & Measurement Magazine* 23.2 (), pp. 4–12. ISSN: 1941-0123. DOI: 10.1109/MIM.2020.9062678 (cit. on p. 1).

[13] B. D. Josephson. "Possible New Effects in Superconductive Tunnelling". In: *Physics Letters* 1.7 (), pp. 251–253. ISSN: 0031-9163. DOI: 10.1016/0031-9163(62)91369-0 (cit. on p. 1).

[14] Y. Cao et al. "Unconventional Superconductivity in Magic-Angle Graphene Superlattices". In: *Nature* 556.7699 (), pp. 43–50. ISSN: 1476-4687. DOI: 10.1038/nature26160 (cit. on p. 2).

[15] P. Coleman. *Introduction to Many-Body Physics*. Cambridge University Press. ISBN: 978-0-521-86488-6. DOI: 10.1017/CBO9781139020916 (cit. on pp. 3, 8, 10, 14).

[16] M. Tinkham. *Introduction to Superconductivity*. 2. ed. International Series in Pure and Applied Physics. New York: McGraw-Hill. 454 pp. ISBN: 978-0-07-064878-4 (cit. on pp. 3, 8).

[17] H. Bruus and K. Flensberg. *Many-Body Quantum Theory in Condensed Matter Physics: An Introduction*. Oxford Graduate Texts. Oxford, New York: Oxford University Press. 466 pp. ISBN: 978-0-19-856633-5 (cit. on pp. 3, 10, 12).

[18] A. I. Larkin and A. A. Varlamov. *Theory of Fluctuations in Superconductors*. Oxford Science Publications 127. Oxford Oxford: Clarendon Press Oxford University Press. ISBN: 978-0-19-852815-9 (cit. on p. 3).

[19] K. H. Bennemann and J. B. Ketterson, eds. *Superconductivity*. Berlin, Heidelberg: Springer Berlin Heidelberg. ISBN: 978-3-540-73252-5. DOI: 10.1007/978-3-540-73253-2 (cit. on p. 3).

[20] N. Witt et al. "Bypassing the Lattice BCS–BEC Crossover in Strongly Correlated Superconductors through Multiorbital Physics". In: *npj Quantum Materials* 9.1 (), pp. 1–10. ISSN: 2397-4648. DOI: 10.1038/s41535-024-00706-7 (cit. on pp. 3, 7).

[21] A. Beekman, L. Rademaker, and J. van Wezel. "An Introduction to Spontaneous Symmetry Breaking". In: *SciPost Physics Lecture Notes* (), p. 011. ISSN: 2590-1990. DOI: 10.21468/SciPostPhysLectNotes.11 (cit. on p. 3).

[22] E. Noether. "Invariante Variationsprobleme". In: *Nachrichten von der Gesellschaft der Wissenschaften zu Göttingen, Mathematisch-Physikalische Klasse* 1918 (), pp. 235–257. URL: https://eudml.org/doc/59024 (cit. on p. 4).

[23] L. D. Landau. "On the Theory of Phase Transitions". In: *Zhurnal Eksperimental'noi i Teoreticheskoi Fiziki* 7 (). Ed. by D. ter Haar, pp. 19–32. DOI: 10.1016/B978-0-08-010586-4.50034-1 (cit. on p. 4).

[24] V. L. Ginzburg and L. D. Landau. "On the Theory of Superconductivity". In: *Zhurnal Eksperimental'noi i Teoreticheskoi Fiziki* 20 (). Ed. by D. ter Haar, pp. 1064–1082. DOI: 10.1016/b978-0-08-010586-4.50078-x (cit. on pp. 4, 6).

[25] N. F. Q. Yuan and L. Fu. "Supercurrent Diode Effect and Finite-Momentum Superconductors". In: *Proceedings of the National Academy of Sciences* 119.15 (), e2119548119. DOI: 10.1073/pnas.2119548119 (cit. on p. 8).

[26] R. Shimano and N. Tsuji. "Higgs Mode in Superconductors". In: *Annual Review of Condensed Matter Physics* 11 (Volume 11, 2020), pp. 103–124. ISSN: 1947-5454, 1947-5462. DOI: 10.1146/annurev-conmatphys-031119-050813 (cit. on p. 8).

[27] L. N. Cooper. "Bound Electron Pairs in a Degenerate Fermi Gas". In: *Physical Review* 104.4 (), pp. 1189–1190. DOI: 10.1103/PhysRev.104.1189 (cit. on p. 8).

[28] L. C. Hebel and C. P. Slichter. "Nuclear Relaxation in Superconducting Aluminum". In: *Physical Review* 107.3 (), pp. 901–902. DOI: 10.1103/PhysRev.107.901 (cit. on p. 9).

[29] L. C. Hebel and C. P. Slichter. "Nuclear Spin Relaxation in Normal and Superconducting Aluminum". In: *Physical Review* 113.6 (), pp. 1504–1519. DOI: 10.1103/PhysRev.113.1504 (cit. on p. 9).

[30] I. Giaever and K. Megerle. "Study of Superconductors by Electron Tunneling". In: *Physical Review* 122.4 (), pp. 1101–1111. DOI: 10.1103/PhysRev.122.1101 (cit. on p. 9).

[31] X. Zhou et al. "High-Temperature Superconductivity". In: *Nature Reviews Physics* 3.7 (), pp. 462–465. ISSN: 2522-5820. DOI: 10.1038/s42254-021-00324-3 (cit. on p. 9).

[32] J. Hubbard and B. H. Flowers. "Electron Correlations in Narrow Energy Bands". In: *Proceedings of the Royal Society of London. Series A. Mathematical and Physical Sciences* 276.1365 (), pp. 238–257. DOI: 10.1098/rspa.1963.0204 (cit. on p. 9).

[33] J. Kanamori. "Electron Correlation and Ferromagnetism of Transition Metals". In: *Progress of Theoretical Physics* 30.3 (), pp. 275–289. ISSN: 0033-068X. DOI: 10.1143/PTP.30.275 (cit. on p. 9).

[34] M. C. Gutzwiller. "Effect of Correlation on the Ferromagnetism of Transition Metals". In: *Physical Review Letters* 10.5 (), pp. 159–162. DOI: 10.1103/PhysRevLett.10.159 (cit. on p. 9).

[35] M. Qin et al. "The Hubbard Model: A Computational Perspective". In: *Annual Review of Condensed Matter Physics* 13 (Volume 13, 2022), pp. 275–302. ISSN: 1947-5454, 1947-5462. DOI: 10.1146/annurev-conmatphys-090921-033948 (cit. on p. 9).

[36] R. Micnas, J. Ranninger, and S. Robaszkiewicz. "Superconductivity in Narrow-Band Systems with Local Nonretarded Attractive Interactions". In: *Reviews of Modern Physics* 62.1 (), pp. 113–171. DOI: 10.1103/RevModPhys.62.113 (cit. on p. 10).

[37] K.-E. Huhtinen. "Superconductivity and Normal State Properties in Flat Bands". Aalto University. URL: https://aaltodoc.aalto.fi/handle/123456789/119970 (cit. on p. 10).

[38] J. J. Kinnunen et al. “The Fulde–Ferrell–Larkin–Ovchinnikov State for Ultracold Fermions in Lattice and Harmonic Potentials: A Review”. In: *Reports on Progress in Physics* 81.4 (), p. 046401. ISSN: 0034-4885. DOI: 10.1088/1361-6633/aaa4ad (cit. on p. 11).

[39] A. Georges et al. “Dynamical Mean-Field Theory of Strongly Correlated Fermion Systems and the Limit of Infinite Dimensions”. In: *Reviews of Modern Physics* 68.1 (), pp. 13–125. DOI: 10.1103/RevModPhys.68.13 (cit. on p. 14).

[40] G. Yang et al. “Structure of Graphene and Its Disorders: A Review”. In: *Science and Technology of Advanced Materials* 19.1 (), pp. 613–648. ISSN: 1468-6996. DOI: 10.1080/14686996.2018.1494493 (cit. on p. 15).

[41] E. Bach. “Parasweep: A Template-Based Utility for Generating, Dispatching, and Post-Processing of Parameter Sweeps”. In: *SoftwareX* 13 (), p. 100631. ISSN: 2352-7110. DOI: 10.1016/j.softx.2020.100631 (cit. on pp. 21, 27).

[42] Y. O. Halchenko et al. “DataLad: Distributed System for Joint Management of Code, Data, and Their Relationship”. In: *Journal of Open Source Software* 6.63 (), p. 3262. ISSN: 2475-9066. DOI: 10.21105/joss.03262 (cit. on p. 27).

[43] C. R. Harris et al. “Array Programming with NumPy”. In: *Nature* 585.7825 (), pp. 357–362. ISSN: 1476-4687. DOI: 10.1038/s41586-020-2649-2 (cit. on p. 27).

[44] P. Virtanen et al. “SciPy 1.0: Fundamental Algorithms for Scientific Computing in Python”. In: *Nature Methods* 17.3 (), pp. 261–272. ISSN: 1548-7105. DOI: 10.1038/s41592-019-0686-2 (cit. on p. 27).

[45] J. D. Hunter. “Matplotlib: A 2D Graphics Environment”. In: *Computing in Science & Engineering* 9.3 (), pp. 90–95. ISSN: 1558-366X. DOI: 10.1109/MCSE.2007.55 (cit. on p. 27).

[46] W. McKinney. “Data Structures for Statistical Computing in Python”. In: Python in Science Conference. Austin, Texas, pp. 56–61. DOI: 10.25080/Majora-92bf1922-00a (cit. on p. 27).

[47] T. pandas development team. *Pandas-Dev/Pandas: Pandas*. Version v2.2.3. Zenodo. DOI: 10.5281/ZENODO.3509134 (cit. on p. 27).

Not cited

[48] F. London. "A New Conception of Supraconductivity". In: *Nature* 140.3549 (), pp. 793–796. ISSN: 1476-4687. DOI: 10.1038/140793a0.

[49] O. Parcollet et al. "TRIQS: A Toolbox for Research on Interacting Quantum Systems". In: *Computer Physics Communications* 196 (), pp. 398–415. ISSN: 0010-4655. DOI: 10.1016/j.cpc.2015.04.023.

[50] S. Peotta and P. Törmä. "Superfluidity in Topologically Nontrivial Flat Bands". In: *Nature Communications* 6.1 (), p. 8944. ISSN: 2041-1723. DOI: 10.1038/ncomms9944.

[51] J. P. Provost and G. Vallee. "Riemannian Structure on Manifolds of Quantum States". In: *Communications in Mathematical Physics* 76.3 (), pp. 289–301. ISSN: 1432-0916. DOI: 10.1007/BF02193559.

List of Symbols

Symbol	Meaning	Definition
$C_{AB}(\tau, 0)$	Correlation function in imaginary time	13